

The Study of Ion Adsorption by Amorphous Blast Furnace Slag

Nilforoushan, Mohammad Reza⁺; Otraj, Sasan*

Faculty of Engineering, Shahrekord University, Shahrekord, I.R. IRAN

Talebian, Nasrien

Faculty of Science, Islamic Azad University, Shahreza Branch, Shahreza, I.R. IRAN

ABSTRACT: *In this study, the blast furnace slag was used as absorbing bed and then, its ionic adsorption was studied. For this reason, various experimental parameters such as pH, contact time and the primary ion concentration were investigated. The remaining concentrations of ions such as; Mn^{2+} and Fe^{2+} in water were measured by atomic adsorption spectroscopy. The chemical and phase composition of slag, before and after ion removal, was investigated. SEM, FTIR, XRD, and EDAX, was used to have a clear understanding of the mechanism of ions removal by slag. The results showed that the removal mechanism of metal ions is carried by adsorption and ion exchange processes. The ionic radius is one of the determining parameters on the process at higher concentration of ions. This study demonstrates that steel slag can be considered as a viable and cost-effective alternative to commercial activated carbon or ion-exchange resins.*

KEY WORDS: *Blast furnace slag, Adsorption, Ionic exchange, Phase composition.*

INTRODUCTION

Slag is a major waste product generated during the steel-making process so that, steel making process in electric arc furnaces generates up to 15 % of slag per ton of steel. Major components of steel mill slag include Ca-silicates, Ca-Al-ferrites, and molten oxides of calcium, iron, magnesium, and manganese. The composition of slag varies upon the type of furnace and charge, the desired grade of steel purity and the furnace operation conditions. Materials to be added to the steel melt directly before the end of the reheating process are not fully embedded in the slag structure, so they can be found in the slag as “free “oxides (CaO, MgO). Compared to blast furnace slag, steelmaking slag shows a considerably

higher content of iron, manganese, and magnesium along with the lower silicon content i.e. higher CaO/SiO₂ ratio, and, finally, it contains almost no sulphur at all. Slag is one of the waste materials that are being widely reused for their useful properties. For example, portion of the separated slag, that does not have an increased content of metallic components, with regard to its properties, can be applied in the construction industry. Furthermore, it was observed that Electric Arc Furnace (EAF) slag can be used as inexpensive absorbing agent in the treatment process for waste waters burdened with heavy metal ion such as Pb²⁺ [1]. When manganese and iron ions are present in water, they may cause different kinds of problems

* To whom correspondence should be addressed.

+ E-mail: m_r_nilforoushan@yahoo.com

1021-9986/13/3/

8/\$2.80

and most importantly health disease. Therefore, slag can be used as absorbing bed for removal of manganese and iron ions from water. This effect can be related to the presence of silicates in the slag composition. It is well known that surfaces of silicate glasses and amorphous structures can be hydrated when will be contact with water containing environments, including normal air [2–7]. Therefore, ionic exchange process can be occurred. Hydration degrades the surface of the glass and may affect glass strength due to interaction of hydrated layer with strength controlling defects [7-9,10]. Although, the phenomenon of glass surface hydration is still not fully understood, most researchers agree that hydration involves several competing processes, the most significant of which are leaching (often referred to as ion exchange) and network dissolution [11–15]. It has been proposed that H₂O moves through the glass in a series of jumps into “doorways” or small interstitial sites [16]. The rate at which this process occurs depends upon the intermolecular distance of the host material matrix compared to the size of the diffusing species [17]. Based on the previous literature [18-21], in the present study, attempt has been made to remove manganese and iron ions from water by steel slag as a cheap industrial by-product, as well as, studying the mechanism of ion removal by several techniques.

EXPERIMENTAL SECTION

Granulated blast furnace slag (GBFS) used was a commercial by-product of the Esfahan Steel Company. It was water jet cooled, hence in mostly amorphous state. The chemical composition of slag was analyzed by X-ray fluorescence. The X-ray fluorescence was Cambridge model XR300. The mineralogy of slag examined by a Bruker Germany ED8 advance diffractometer using monochromatic Cu K α radiation with a wavelength 1.5406 Angstrom. The pH measurements made by using a pH meter (TM-6). The micro structural and EDAX analysis was done by a Korean made SEM from Seron Technology model AIS 2100. The hydration behavior of slag was followed by FTIR, model impact 400p Nicolet. A few milligrams of sample was mixed with KBr and pressed to form a tablet. The stock solutions were prepared using analytical grade metal salt manufactured by Merck Company. Iron in the form of FeSO₄.7H₂O and manganese in the form of MnSO₄.H₂O. The concentrations of metals after ion exchange reactions

Table 1: Chemical composition of different steel slags.

Chemical composition wt%	GBFS
CaO	35.86-36.30
MgO	11.23-11.60
SiO ₂	36.51-36.21
FeO	0.90-0.50
Al ₂ O ₃	9.95-9.98
MnO	1.10-0.71
S	1.07-0.86
Pb	Not detected
Zn	Not detected
TiO ₂	3.30-2.82
V ₂ O ₅	0.08-0.07

were conducted by atomic absorption spectrometer model Perkin Elmer model AAnalyst 300 (AAS). Four different standard solutions were prepared in order to get a linear standard curve, introduced by manufacturer of the Atomic Absorption instrument. The ionic concentration ranged between 2 and 10 mg/lit, based on the concentration of metals. Slag was fractionated, rinsed with distilled water to remove fines, dried at 105°C and stored in a bank. Column experiments were conducted in a glass column (5 cm ID) packed with GBFS. Two different particle sizes of slag were used (0.25–0.50 and 0.50–2.5mm). The apparent density of slag was measured as 1.27 g/cm³. The slag bed height was 31 cm. Iron and manganese containing solutions were passed downward through the column. At requires time intervals, 15mL of the effluent samples were collected regularly and analyzed without previous filtration. Every set of experiments was done twice in order to investigate its reproducibility.

RESULTS AND DISCUSSIONS

Chemical analysis of slag.

Chemical characterization of slag (Table 1), the adsorbent used in the present study shows that, its main constituents are silica (36.35%) and lime (36.02%). Oxides of other metals are present in traces. These results are the mean chemical composition of various samples of slag produced in two weeks. Based on the results, slag is mostly composed of Calcium and magnesium oxide (11.42) which makes it a basic slag.

Table 2: Adsorption of Mn^{2+} ions by GBFS at different time.

Time/h	mg/L	% removal	mg/L	% removal	mg/L	% removal
0	2	0	5	0	10	0
0.5	0.045	97.75	0.075	98.50	0.093	99.07
1	0.045	97.75	0.071	98.58	0.091	99.09
2	0.045	97.75	0.067	98.66	0.085	99.15
4	0.041	99.95	0.053	98.94	0.062	99.38
8	0.037	99.96	0.052	98.96	0.043	99.57
24	0.033	99.97	0.051	98.98	0.027	99.73
48	0.028	99.98	0.040	99.20	0.026	99.74

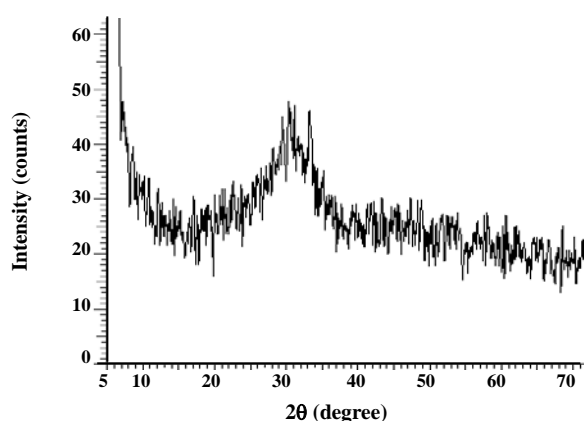


Fig. 1: X-ray diffraction pattern of GBFS.

Measurement of pH of slag in pure water

The pH changes during hydration of slag were measured at different time intervals. Relatively high and constant pH values (8.9–9.2) were observed for GBFS. It is due to hydrolysis reaction that the slag can slowly release hydroxyl ions in the aqueous phase. Since the distilled water has an enhanced H^+ content, the hydrolysis was probably accompanied by an exchange reaction between the calcium ions of the slag and the hydrogen ions.

According to the previous investigations from interruption experiments, it has also been suggested that these processes can occur both on the slag surface and in its bulk [22].

Mineralogical properties of slag

The mineralogical characterization of slag shows (Fig. 1) that it is mostly composed of amorphous phase, due to its rapid cooling from the melt.

Effect of contact time and initial concentration of Mn^{2+} ions

Effect of contact time and concentration on the removal of Mn(II) has been shown in Table 1. Based on the results, by varying concentration of Mn(II) in solution from 2 to 10 mg/L, the removal (%) increases from 97.75 to 99.07% at 25 °C. The results also shows sharp rise in removal of Mn (II) in initial stages. Then gradually it attains equilibrium in 24 hours and becomes constant. The process of Mn (II) removal on slag is highly concentration dependent. High removal of Mn (II) in this range of concentration has lot of industrial significance as in most cases the waste waters and industrial effluents have been reported to have lower concentrations of metallic species including that of Mn(II) [29]. Slag may also be used in the cases where the concentration of Mn (II) is high.

Effect of contact time and initial concentration of Fe^{2+} ions

The results of concentration and its contact time of Fe(II) ions with slag are shown in Fig. 2. According to this figure, the removal of Fe(II) in solution is concentration dependant and by varying concentration from 2 to 10 mg/L, the removal (%) increased by ion concentration. This figure shows sharp rise in removal of Fe(II) in initial stages. Then it gradually attains equilibrium in 120 min and becomes relatively constant. The removal process is highly concentration dependent. Although in comparison, there is not much difference on the removal rate of various concentrations of Mn(II) ions, but in this case better removal shows at higher concentration of Fe(II).

Removal rate of total metal ion by GBFS

As described above, total metal remained in water to some extent depends on the higher pH's. F_f indicates the total ion concentration in water, and F the total ion concentration at each sampling point. This relationship may be written as follows:

$$\ln \left\{ \frac{(F - F_f)}{(F_0 - F_f)} \right\} = -\lambda' \cdot z$$

this equation is rewritten as follow:

$$dF / dt = -\lambda' \cdot v \cdot (F - F_f) = -\lambda \cdot (F - F_f)$$

Where F is the total metal concentration (mg/L); F_0 the total iron concentration in water after reaction (mg/L); F_o the total ion concentration in water before reaction (mg/L); λ' the total metal removal coefficient (m^{-1}); λ is the total metal removal rate coefficient (h^{-1}) and is the filtration or removal rate (m/h) [23].

The removal rate for both ions by slag was calculated. The results are graphically shown in Figs. 3 & 4. According to the mineralogical composition of GBFS, by hydration of slag, the calcium ion leaches into the solution and leaves a negatively charged network and the negative surface of network adsorbs positive ions from the solution. The smaller ion adsorbs and diffuses into the network more easily. In this case iron ions diffuse to the network faster than manganese ions due to its lower ionic radii (Table 3) and also compared to calcium ions.

Comparison of the results (shown in Figs. 3&4) reveals that, the removal rate of iron ions by GBFS especially at higher concentration is faster than manganese ions and it follows a normal trend too. Also in all cases for manganese ions, the removal rate decreases after 24 hours. This is possibly due to the surface saturation of the network that prevents further diffusion of manganese ions.

Investigations of slag hydration by FT-IR

FTIR spectra is a useful tool to identify functional groups in a molecule, as each specific chemical bond often has a unique energy adsorption band, and can obtain structural and bond information on a complex to study the strength and the fraction of hydrogen bonding and miscibility [24]. The FTIR spectra of GBFS before and after hydration were taken at (KBr) ν : 400–4000 cm^{-1} , the spectra are shown in Figs. 5 & 6 respectively. In the pattern taken from slag before hydration (shown in Fig.5), there is a very intense peak due to the stretching vibration of Si-O bond at 1021 cm^{-1} . By soaking of slag

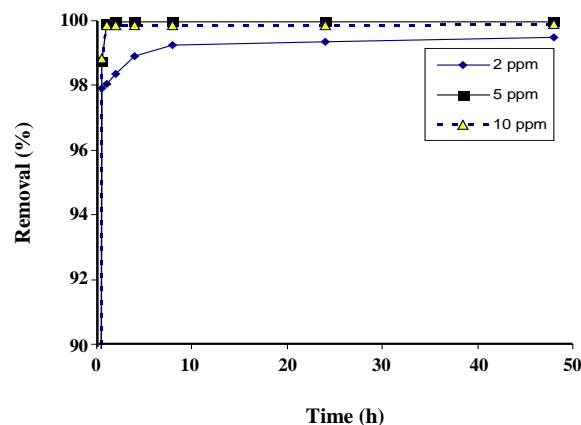


Fig. 2: Adsorption of various concentrations of Fe(II) ions by GBFS.

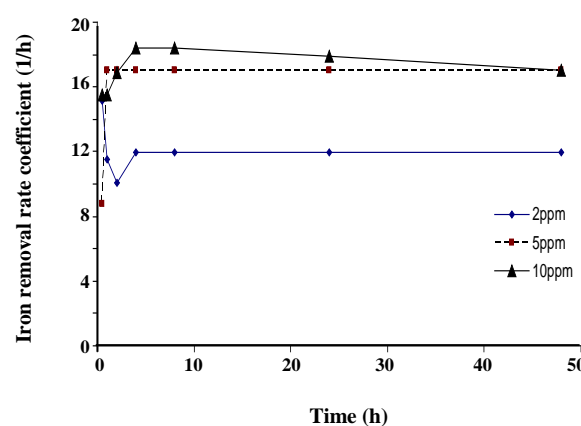


Fig. 3: Comparison of the Fe(II) removal rate coefficient with respect to Iron ion concentration by GBFS.

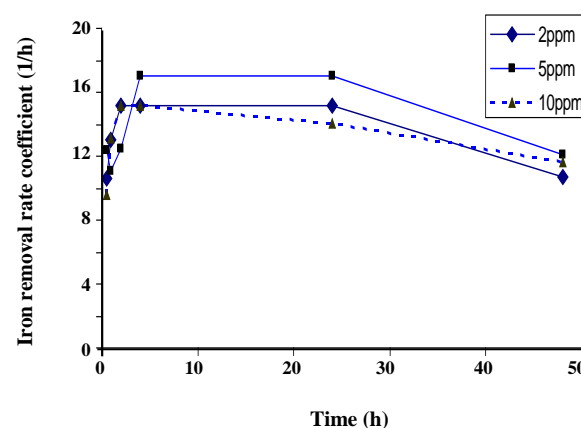


Fig. 4: Adsorption of various concentrations of Fe(II) ions by GBFS.

Table 3: Ionic radii of cations.

Cation	Radii / Å°	Radii / pm
Ca ²⁺	1	100
Mn ²⁺	0.67	67
Fe ²⁺	0.61	61

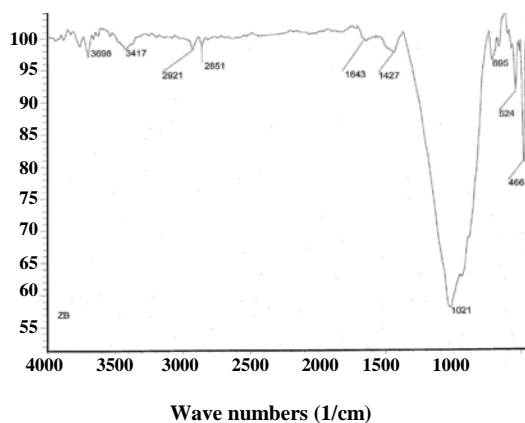


Fig. 5: FTIR Spectra of GBFS (ZB) before hydration.

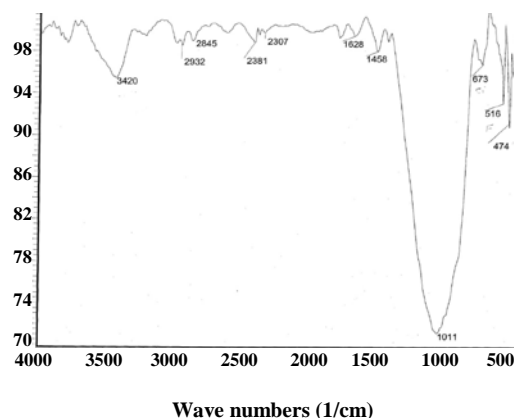
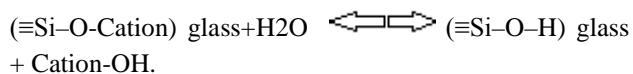


Fig 6: FTIR Spectra of GBFS (ZBH) after hydration.

in water for 24 hours, it becomes hydrolyzed and a new peak due to its surface hydration appears at around 3420cm^{-1} attributed to the stretching vibration of $-\text{OH}$, which has been absorbed on the network. Its pattern is shown in Fig. (6). Comparison of two FTIR patterns reveals that the intensity of the peak at 1021 cm^{-1} decrease possibly due to the hydrolyze of some of the Si-O bonds in the network. Some of the results of examination of steel slag by FTIR have been previously published in literature [25].

This kind of behavior is due to the amorphous nature of slag and may be interpreted as follows; the ion exchange reaction of glass with water can be written as



This reaction is controlled by the counter diffusion of protons (probably as H_3O^+) from water which replace cations in the glass structure e.g. cations bonded to Non-Bridging Oxygens (NBO), which in this case were calcium ions [26-27]. These reaction initiates soon after the beginning of the immersion tests [28], which has been previously interpreted as a silicate gel layer [29]. This behavior may be interpreted by increasing in pH of water due to the formation of $\text{Ca}(\text{OH})_2$.

Microstructural investigations of steel slag

The electron micrograph of taken from the surface of slag (shown in Fig. 8) reveals that the slag has an amorphous and vesicular structure due to its rapid cooling from the melt. These results are in agreement with the results taken from X-ray diffraction pattern.

Investigations on the mineralogical changes of slag during hydration

In order to have a clear understanding of mineralogical changes of slag before and after hydration, the X-ray diffraction pattern of slag was taken before and after hydration in pure distilled water. The following peaks were recognized in the patterns shown in Fig. 7 from the sample before hydration named ZB. In this pattern, a broad peak from $2\theta = 20-40^\circ$ due to the glass formation and two relatively sharp peaks at $2\theta = 24.1$ and 38° respectively, due to the formation of Melilite [Me] ($\text{Ca}_8\text{Al}_2\text{Mg}_3\text{Si}_7\text{O}_{28}/8\text{CaO}\cdot\text{Al}_2\text{O}_3\cdot 3\text{MgO}\cdot 7\text{SiO}_2$), and also a peak attributed to the formation of Akermanite [AK] ($\text{Ca}_2\text{MgSi}_2\text{O}_7$) at $2\theta = 31.2^\circ$ was recognized. By hydrating of slag (sample named ZBH), both peaks of Melilite disappeared and new peaks at $2\theta = 34.1$ due to the formation of Portlandite [Po] [$\text{Ca}(\text{OH})_2$], and another one at $2\theta = 31.9$ attributed

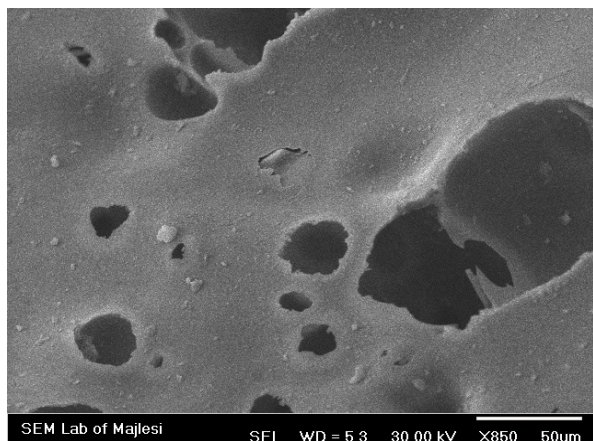


Fig. 7: Microstructure of GBFS slag.

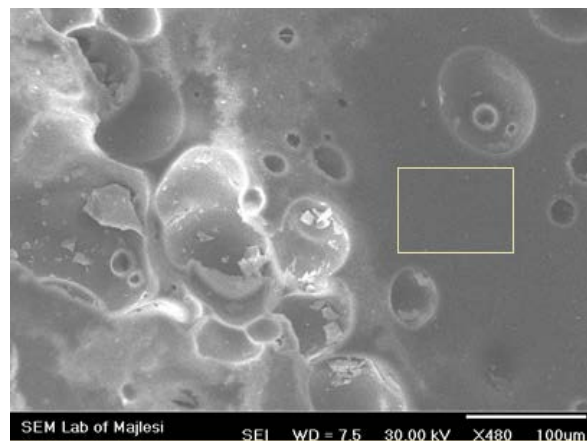


Fig. 9: Selected area of GBFS surface used for EDAX analysis after Mn and Fe removal.

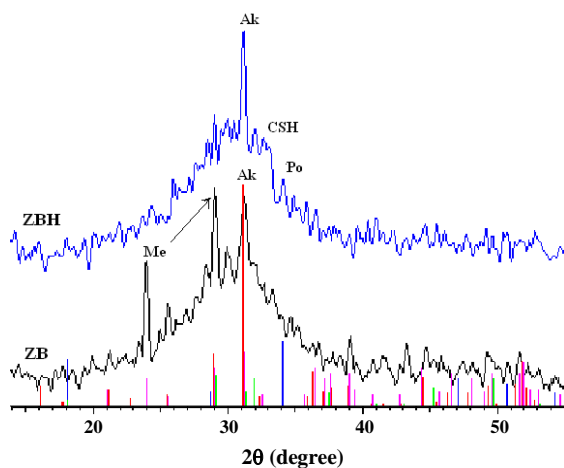


Fig. 8: X-ray diffraction pattern of GBFS before and after hydration.

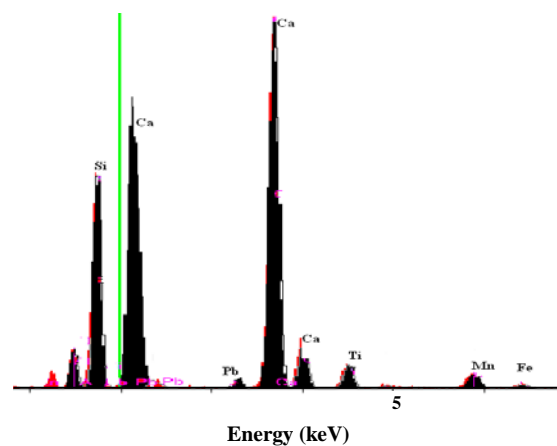


Fig. 10: EDAX analysis of GBFS after Mn and Fe removal.

to the formation of Calcium Silicate Hydrate [CSH] ($\text{Ca}_8\text{Al}_2\text{Mg}_3\text{Si}_7\text{O}_{28}/8\text{CaO}\cdot\text{Al}_2\text{O}_3\cdot 3\text{MgO}\cdot 7\text{SiO}_2$) was appeared. Since Melilite is a calcium rich phase, by hydrating of slag, it dissolves and the alkali metals especially calcium ions leaches out of the network and leaves a negatively charged surface, which adsorbs hydrogen or other positively charged ions available in the solution through an ion exchange reaction.

Surface analysis of slag after ion removal by EDAX.

In order to investigate the adsorption of ions by network, the surface of GBFS after soaking in 10ppm solution of both ions were analyzed by EDAX. The selected area which was analyzed together with its EDAX result are shown in Figs. 9&10 respectively.

There are two weak peaks attributed to the elements of Mn and Fe. Comparison of the concentration of these ions with one previously showed in the chemical analysis of slag in Table 1, reveals that the concentration of these two ions is much higher than what was expected. This may be due to the ion exchange reactions taking place on the surface of slag.

CONCLUSIONS

The type of process explained in this paper can be used for treating of water, containing relatively high manganese and iron concentrations.

The removal rate of iron ions by GBFS especially at higher concentration is faster than manganese ions which can be due to the difference of their ionic radii.

The mechanism of ion removal by amorphous slag is through ion exchange reactions on negatively charged network formed during hydrolyzing in water.

This type of slag can remove various concentrations of iron and manganese ions from water, but the trend of ionic removal follows a special order based on increasing ionic concentration of solution.

The technique has some advantages, viz., low manufacturing cost, almost nil recurring cost, no electricity requirement, and simplicity in use.

Received : Mar. 13, 2013 ; Accepted : Apr. 14, 2014

REFERENCES

- [1] Nilforoushan M.R., Otroj S., [Absorption of Lead Ions by Various Types of Steel Slag](#), *Iran. J. Chem. Chem. Eng. (IJCCE)*, **27**: 69-75 (2008).
- [2] Doremus R.H., Mehrotra Y., Lanford W.A., Burman C., [Reaction of Water with Glass: Influence of a Transformed Surface Layer](#), *J. Mater. Sci.*, **18**: 612-622 (1983).
- [3] Schnatter K.H., Doremus R.H., Lanford W.A., [Hydrogen Analysis of Soda-Lime Silicate Glass](#), *J. Non-Cryst. Solids*, **102**: 11-15 (1988).
- [4] Scholze H., [Non-Cryst. Solids J., Durability Investigation of Siliceous Man-Made Mineral Fibers: a Critical Review](#), **102**: 1-17 (1998).
- [5] Bunker B.C., [Molecular Mechanisms for Corrosion of Silica and Silicate Glasses](#), *J. Non-Cryst. Solids*, **179**: 300-308 (1994).
- [6] Cailleteau C., Angeli F., Devreux F., Gin S., Jestin J., Jollivet P., Spalla O., [Insight Into Silicate- Glass Corrosion Mechanisms](#), *Nat. Mater.*, **7**: 978-983 (2008).
- [7] Davis K.M., Tomozawa M., [Water Diffusion into Silica Glass: Structural Changes in Silica Glass and Their Effect on Water Solubility and Diffusivity](#), *J. Non-Cryst. Solids*, **185**: 203-220 (1995).
- [8] Griffiths D.R., Feuerbach A.M., [The Conservation of Wet Medieval Window Glass: A Test Using an Ethanol and Acetone Mixed Solvent System](#), *JAIC*, **40**: 125-136 (2001)
- [9] Koenderink G.H., Brzesowsky R.H., Balkenende A.R., [Effect of the Initial Stages of Leaching on the Surface of Alkaline Earth Sodium Silicate Glasses](#), *J. Non-Cryst. Solids*, **262**: 80-98 (2000).
- [10] Pavelchek E.K., Doremus R.H., [Static Fatigue in Glass - A Reappraisal](#), *J. Non-Cryst. Solids*, **20**: 305-321 (1976).
- [11] Vilarigues M., da Silva R.C., [The Effect of Mn, Fe and Cu Ions on...and IR Spectroscopy](#), *J. Non-Cryst. Solids*, **352**: 5368-5375 (2006).
- [12] Nascimento E.M., Lepienski C.M., [Mechanical Properties of Optical Glass Fibers Damaged by Nanoindentation and Water Ageing](#). *J. Non-Cryst. Solids*, **352**: 3556-3560 (2006).
- [13] Rana M.R., Douglas R.W., [The Structure of Leached Sodium Borosilicate glass](#), *Phys. Chem. Glasses*, **2**: 196- (1961)
- [14] Doremus R.H., in: M. Tomozawa, R.H. Doremus (Eds.), "Glass II", Vol. 17, (Academic, New York, pp. 41-69 (1979).
- [15] Perera G., Doremus R.H., [Dissolution Rates of Commercial Soda-Lime and Pyrex Borosilicate Glasses: Influence of Solution pH](#), *J. Am. Ceram. Soc.*, **74**: 1554-1558 (1991).
- [16] Doremus R.H., "Diffusion and Reactive Molecules in Solids and Melts", (Wiley Interscience, New York, (2002)
- [17] Liritzis I., [A New Obsidian Hydration Dating Method: Analysis and Theoretical Principles](#), *Archaeometry*, **48**: 533-547 (2006).
- [18] Sharma Y.C., Umaa A., Singh b S.N., Paras c, F. Goded, [Fly Ash for the Removal of Mn\(II\) from Aqueous Solutions and Wastewaters](#), *J. Chem. Eng.*, **132**: 319-327 (2007).
- [19] Katsoyiannis I.A., Zouboulis A.I., [Biological Treatment of Mn\(II\) and Fe\(II\) Containing Groundwater: Kinetic Considerations and Product Characterization](#), *J. Wat. Res.*, **38**:1922-1932 (2004).
- [20] Roccaro P., Barone C., Mancini G., Vagliasindi F.G.A., [Removal of Manganese from Water Supplies Intended for Human Consumption: a Case Study](#), *J. Desalin.*, **210**: 205-214 (2007).
- [21] Gu Z., Fang J., Deng B., [Preparation and Evaluation of GAC-Based Iron Containing Adsorbents for Arsenic Removal](#), *Environ. Sci. Technol.*, **39**, 3833-3843 (2005).
- [22] Bong-Yeon Cho, [Iron Removal Using an Aerated Granular Filter](#), *Process Biochemistry*, **40**: 3314-3320 (2005).

- [23] Dong J., Ozaki Y., FTIR and FT-Raman Studies of Partially Miscible Poly (methylmethacrylate)/poly(4-vinyl- phenol) Blends in Solid States, *J. Macromolecules*, **30**: 286-292 (1997).
- [24] Zhou D., Zhang L., Zhou J., Guo S., Cellulose/Chitin Beads for Removal of Heavy Metals in Aqueous Solution, *J. Wat. Res.*, **38**: 2643-2651 (2004)
- [25] Ojovan M. I., Lee W.E., "An Introduction to Nuclear Waste Immobilization", (Elsevier Science Publishers B.V., Amsterdam, (2005).
- [26] Ojovan M.I., Pankov A., Lee W.E., The Ion Exchange Phase in Corrosion of Nuclear Waste Glasses, *J. of Nuclear Mater.*, **358**, 57-68 (2006).
- [27] Vilarigues M., da Silva R.C., The effect of Mn, Fe and Cu Ions on Potash-Glass Corrosion, *J. Non-Cryst. Solids*, **355**, 1630-1637 (2009).
- [28] Tournié A., Ricciardi P., Colomban Ph., Glass Corrosion Mechanisms: a Multiscale Analysis, *Solid State Ionics*, **179**: 2142-2151 (2008).
- [29] Tadjiev D.R., Hand R.J., Zeng P., Surface Hydration and Nanoindentation of Silicate Glasses, *Mat. Let.*, **64**: 1041-12049 (2010).